Evaporation residue measurements of compound nuclei in the $A \approx 200$ region

P. Jisha,[1,*] A. M. Vinodkumar,[1] B. R. S. Babu,[1] S. Nath,[2] N. Madhavan,[2] J. Gehlot,[2] A. Jhingan,[2] T. Banerjee,[2,†] Ish Mukul,[2,‡] R. Dubey,[2,§] N. Saneesh,[2] K. M. Varier,[3] E. Prasad,[4] A. Shamlath,[4] P. V. Laveen,[4] and M. Shareef[4]

[1]*Department of Physics, Calicut University, Calicut 673 635, India*

[2]*Nuclear Physics Group, Inter University Accelerator Centre, Aruna Asaf Ali Marg, New Delhi 110067, India*

[3]*Department of Physics, University College, Palayam, Thiruvananthapuram 695034, Kerala, India*

[4]*Department of Physics, School of Physical Sciences, Central University of Kerala, Kasaragod 671316, India*

(Received 12 November 2019; accepted 24 January 2020; published 27 February 2020)

Background: The onset of a noncompound nuclear fission (NCNF) process such as quasifission was already predicted for heavy symmetric systems with the charge product greater than 1400. However, quasifission is observed indeed in very asymmetric reactions forming ^{216}Ra with much lower charge product($\approx$700). A comprehensive idea about the dependence of quasifission on entrance channel mass asymmetry with smaller charge product is still missing. A clear understanding is vital in the production of superheavy elements.

Purpose: To investigate limiting value of mass asymmetry near the Businaro-Gallone point where the fusion probability starts to deviate from unity.

Method: Evaporation residue (ER) cross sections were measured for ^{16,18}O + ^{181}Ta reactions at $E_{\rm lab} = 68$–110 MeV using a recoil mass spectrometer and compared with coupled-channel and statistical model calculations.

Results: Below the Coulomb barrier region, coupled channel calculations reproduced the excitation functions of both ^{16,18}O + ^{181}Ta reactions. Further, statistical model calculations with the same fission barrier scaling factor $k_f = 0.95$ reproduced the experimental ER cross-section energies above the Coulomb barrier.

Conclusions: We do not observe any significant signature of fusion suppression in ER excitation functions of ^{18}O + ^{181}Ta reaction, in comparison with that of ^{16}O + ^{181}Ta. This may be attributed to the high resemblance in mass asymmetry and other structural properties of these systems. A fission barrier scaling factor, $k_f = 0.95$ used in the statistical model calculations for both systems, explains the experimental ER and fission cross sections, indicating the absence of any NCNF.

DOI: 10.1103/PhysRevC.101.024611

I. INTRODUCTION

Measurement of evaporation residue (ER) cross sections is one of the principal methods to investigate the fusion suppression observed in heavy systems. Prior understanding of the causes of the fusion hindrance from heavy-ion reactions is crucial in superheavy element (SHE) production [1,2]. The ER measurements in the $A \approx 200$ region may allow us to find the triggering point of noncompound nuclear fission (NCNF) reactions and further help in explaining the reasons for fusion hindrances [3–6].

Fusion reactions near and below the Coulomb barrier region are extensively studied and interpreted in terms of coupling of relative motions of colliding nuclei with various internal degrees of freedom, such as static deformation, collective surface vibrations, transfer channels, etc. [7]. However, the barrier penetration model properly coupled with these degrees of freedom is inadequate to explain the fusion hindrance above the barrier energies with massive partners [8–10]. In heavy-ion collisions, at higher energies, even after capture there exists a probability for projectile-target system to reseparate before complete equilibration (quasifission [11,12], fast fission, etc.) and thereby to reduce the compound nucleus formation probability ($P_{\rm CN}$). The corresponding ER cross sections at higher energies is weakly sensitive to nuclear potentials [6,13], and usually calculated with standard statistical model (SSM) parameters such as ratio of the level densities in fission and evaporation channels (a_f/a_n), fission barrier scaling factor (k_f), and ground state shell correction (δW_{gs} [14]). Usually, SSM calculations are carried out with a set of parameters [10,15]. Most of them being default parameters, a deviation of $P_{\rm CN}$ from unity indicates the presence of fusion suppression for systems forming the same compound nucleus (CN). In SSM calculations, fission and ER excitation functions of systems forming the same compound nuclei are reproduced with the same parameters of the nuclear potential k_f and with different $P_{\rm CN}$ [6,16]. However, there is no clear understanding of the factors affecting the $P_{\rm CN}$ [17]. Different models assume various factors such as mass asymmetry, or elongation, or both, in a time-independent or dynamical approach to approximate the value of $P_{\rm CN}$ [18,19]. Also, their predictions differ by orders of magnitude [20,21].

*jisha_dop@uoc.ac.in

†Flerov Laboratory of Nuclear Reactions (FLNR), Joint Institute for Nuclear Research (JINR), Dubna 141980, Russia.

‡Present address: TRIUMF, 4004 Wesbrook Mall, Vancouver, British Columbia, Canada V6T 2A3.

§Present address: iThemba LABS, National Research Foundation, PO Box 722, 7129 Somerset West, South Africa.

Studies on the ER excitation function measurements of ^{219,221}Ac compound nuclei reported the presence of quasifission (QF) in ^{16}O induced reactions [6]. Again, the ^{216}Ra compound nucleus showed a marked suppression in ER formation, for very asymmetric combinations of colliding nuclei [5,22–24]. Further, several observations reported the presence of QF in the preactinide region for very asymmetric combinations of colliding nuclei [3,4,13,25–28]. Corradi and coworkers [13,25] observed a fusion suppression effect in very asymmetric reactions leading to the preactinide nucleus ^{213}Fr. Further, QF is also observed in reactions forming less fissile ^{210}Rn [3,4], ^{202}Po [26], and ^{202}Pb [27,28] nuclei with close mass asymmetry in the reaction entrance channel. Recently, a systematic analysis by Banerjee *et al.* [29] on fission and ER excitation functions in the mass region 170–220 predicted some approximate boundaries for fusion suppression near the Businaro-Gallone (BG) point [30].

Near the Businaro-Gallone point, which is the highest of all conditional saddle points, systems with mass asymmetry (α) values less than $\alpha_{\rm BG}$ (critical value of mass asymmetry) advance to quasifission. Otherwise, they proceed to CN formation [30]. Among several projectile and target combinations leading to the same CN, for systems with quasifission, the measured fission cross section will be the sum of compound and noncompound nuclear fission cross sections. For systems forming the same CN, Sagaidak and co-workers [23,25] considered the fission barrier scaling factor of the most asymmetric system as k_f, and explained the measured ER and fission cross sections for all others by varying $P_{\rm CN}$. Also, there are attempts to use an excitation energy dependant fission barrier instead of a single value [31,32]. The ER cross sections of ^{19}F + ^{194}Pt forming ^{213}Fr compound nuclei are explained through a fission barrier scaling factor $k_f = 0.78$ [25]. This value of k_f is remarkably smaller than that of the ^{16}O induced reaction ($k_f = 0.82$ [13]) forming the same CN. To use the same fission barrier scaling factor, for reactions forming the same compound nuclei (^{16}O + ^{197}Au and in ^{19}F + ^{194}Pt) Sagaidak *et al.* [25] reduced the $P_{\rm CN}$ value of the latter from 1 to 0.75. This reduction in $P_{\rm CN}$ can be considered as evidence for fusion suppression in ^{19}F + ^{194}Pt. To have a better understanding of the starting point of NCNF processes in the Fr compound nucleus near the BG point, Corradi *et al.* [13] considered ^{18}O + ^{197}Au and ^{9}Be + ^{209}Bi reactions which form ^{215,218}Fr compound nuclei. For both reactions, they obtain a good agreement between experiment and SSM calculation with $k_f = 0.85$ irrespective of their neutron number ($N_{\rm CN} = 128$ and 131). For the reactions mentioned above, which form Fr compound nuclei, $\frac{\alpha}{\alpha_{\rm BG}} < 1$ except for ^{9}Be + ^{209}Bi. This value of $\frac{\alpha}{\alpha_{\rm BG}} < 1$ predicts a probable presence of quasifission in these reactions. Among these reactions, ^{19}F + ^{194}Pt forming ^{213}Fr could be explained with a $P_{\rm CN} < 1$. However, for all others forming Fr compound nuclei, $P_{\rm CN} = 1$ was found suitable. This indicates that the role of mass asymmetry on fusion suppression dominates in less asymmetric systems forming Fr compound nuclei, when the ^{19}F beam is used in comparison with other lighter beams. Further, theoretical calculations on less fissile systems like ^{200}Pb using the dinuclear system (DNS) model, Nasirov et al. [33] point to a relevant fusion suppression in ^{19}F induced reactions (^{19}F + ^{181}Ta), in comparison with that of ^{16}O induced (^{16}O + ^{184}W). Also, Banerjee *et al.* [29], in their studies on systematics, observed a fusion probability less than 1 for ^{19}F + ^{181}Ta and 1 for ^{16}O + ^{184}W. However, for the same reactions Sagaidak *et al.* [34] introduced the same scaling factor $k_f = 0.85$, with $P_{\rm CN} = 1$, which clearly indicates an absence of fusion suppression in these systems. Thus, we can see that the works of Sagaidak *et al.* [34] contradicts the observations of DNS model predictions [33] and of the Banerjee *et al.* [29] study. Existing experimental data is not sufficient to have a clear understanding on fusion suppression probabilities, in the reactions induced by light projectiles like ^{19}F.

Accordingly, it is essential to have more experimental data in this region for a better understanding of the interplay between CN formation and subsequent disintegration into competing reaction channels. In the present work, we report the results of ^{16,18}O + ^{181}Ta which form compound nuclei ^{197,199}Tl, and their ER excitation function measurements near and above the Coulomb barrier energies using a mass spectrometer. Among this, ^{18}O + ^{181}Ta has $\alpha < \alpha_{\rm BG}$, which indicates the probable presence of NCNF. Further, a comprehensive comparison of the present work with ^{19}F + ^{180}Hf ($\alpha < \alpha_{\rm BG}$) reaction [35] which forms ^{199}Tl was made to understand the fusion-suppression probabilities.

The present work is organized as follows. Section II discusses the experimental setup and procedure followed by Sec. III, which describes in detail the analysis performed. Section IV includes details of coupled channel and statistical model calculations, comparison of these calculations with our experimental data, and their possible implications. The summary and conclusion are given in Sec. V.

II. EXPERIMENTAL DETAILS

The experiments were carried out at the 15 UD Pelletron accelerator facility of IUAC, New Delhi. Pulsed beams of ^{16,18}O with pulse separation 4 μs were bombarded on an ^{181}Ta target of thickness ≈170 μg/cm^2 with ≈20 μg/cm^2 carbon backing. ER excitation function measurements were carried out in 2-MeV energy steps at laboratory beam energies ranging between 68 and 110 MeV. ERs were separated from the profound primary beam background by the Heavy Ion Reaction Analyzer (HIRA) [36] and were transported to its focal plane (FP). The HIRA spectrometer is ≈8.8 m in length, and was operated at 0° with respect to the beam direction with an acceptance of 10 msr. Two silicon surface barrier detectors of an active area of 50 mm^2 each with a collimator diameter 1 mm were placed at a distance of 95.6 mm from the target, in the sliding-seal scattering chamber at ±15° with respect to the beam direction. These detectors serve as monitor detectors for absolute normalization of ER cross sections. They are also used in focusing the beam, by looking at the yields from both the detectors. A 30-μg/cm^2 C foil was kept at 10 cm downstream from the

target to reset the ER charge state. At the FP of HIRA, a two-dimensional (2D) position sensitive multiwire proportional counter (MWPC) [37] of active area 150×50 mm^2 was used to detect the ERs.

III. DATA ANALYSIS

The total ER cross section was calculated using the equation

$$\sigma_{\mathrm{ER}} = \frac{Y_{\mathrm{ER}}}{Y_{\mathrm{norm}}} \left(\frac{d\sigma}{d\Omega}\right)_{\mathrm{Ruth}} \Omega_{\mathrm{norm}}(1/\epsilon_{\mathrm{HIRA}}) \qquad (1)$$

where Y_{ER} is the number of ERs detected at the FP of the HIRA, Y_{norm} is the number of scattered beam particles detected by any of the normalization detectors, $(\frac{d\sigma}{d\Omega})_{\mathrm{Ruth}}$ is the differential Rutherford-scattering cross section in the laboratory system, Ω_{norm} is the solid angle subtended by the normalization detectors, and ϵ_{HIRA} is the average ER transmission efficiency of HIRA. Among the parameters mentioned above, one of the essential factors in the operation of any recoil mass separator is its transmission efficiency. For proper planning and execution of the experiment with a recoil separator, it is necessary to estimate the transmission efficiency of the system accurately. Several evaporation channels are possible for a single beam energy. Usually, HIRA is set for the most dominant channel. Thus transmission efficiency will be different for different exit channels. Considering all these, measuring efficiencies for all exit channels of each E_{lab} will be a tedious task. So we relied on a Monte Carlo code TERS [38] for efficiency calculation. We have calculated the efficiency for all channels (which contribute more than ≈1% of total ER cross section) using TERS and estimated ϵ_{HIRA} for each energy by taking the weighted average of all efficiencies over total ER. The relative population of each channel for calculating

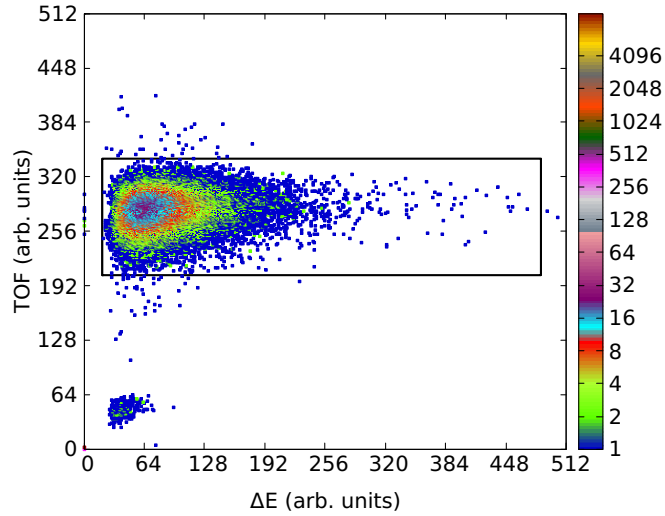

FIG. 1. Scatter plots between ΔE and TOF of the events recorded at the focal plane of HIRA for ^{16}O + ^{181}Ta at 94.0 MeV E_{lab} ($E_{\mathrm{c.m.}} = 86.15$ MeV).

TABLE I. Measured evaporation residue cross sections (σ_{ER}) for ^{16,18}O + ^{181}Ta reactions. Tabulated energies are in the center of mass systems. Here the sum of statistical and systematic errors are quoted as the total error in the measurement.

^{16}O + ^{181}Ta			^{18}O + ^{181}Ta		
$E_{\mathrm{c.m.}}$ (MeV)	E^* (MeV)	σ_{ER} (mb)	$E_{\mathrm{c.m.}}$ (MeV)	E^* (MeV)	σ_{ER} (mb)
100.88	76.04	940.69 ± 108.65	99.90	78.73	983.80 ± 114.77
98.95	74.12	977.64 ± 111.06	98.16	77.00	988.03 ± 114.40
97.26	72.42	961.87 ± 107.36	96.29	75.12	1001.38 ± 112.37
95.44	70.61	998.10 ± 113.22	94.43	73.27	1033.99 ± 120.63
93.58	68.74	982.69 ± 108.19	92.61	71.45	938.18 ± 105.72
91.68	66.84	973.62 ± 108.37	90.84	69.68	945.45 ± 110.45
89.89	65.06	870.23 ± 96.57	88.85	67.69	958.90 ± 111.61
88.00	63.16	787.40 ± 86.62	87.19	66.03	858.38 ± 99.17
86.15	61.31	764.81 ± 81.16	85.24	64.08	835.81 ± 90.47
84.30	59.46	737.20 ± 80.37	83.57	62.41	747.94 ± 81.75
82.47	57.63	621.61 ± 66.96	81.74	60.58	783.18 ± 91.46
80.73	55.90	607.28 ± 67.92	79.79	58.62	681.49 ± 77.97
78.71	53.87	533.61 ± 56.41	78.11	56.95	618.79 ± 70.35
77.00	52.17	454.07 ± 48.71	76.29	55.13	613.97 ± 69.02
75.18	50.35	384.55 ± 41.89	74.49	53.33	453.75 ± 48.16
73.21	48.37	281.82 ± 30.51	72.63	51.47	307.67 ± 33.46
71.36	46.52	195.27 ± 20.84	70.61	49.45	206.15 ± 22.67
69.64	44.81	101.05 ± 15.54	69.01	47.85	131.33 ± 14.29
67.83	43.00	47.63 ± 5.24	67.12	45.95	51.02 ± 5.62
65.95	41.11	16.14 ± 1.78	65.30	44.13	17.41 ± 1.96
64.11	39.28	2.93 ± 0.37	63.33	42.17	3.44 ± 0.41
62.33	37.50	0.205 ± 0.04	61.51	40.35	0.39 ± 0.06
			59.85	38.68	0.10 ± 0.02

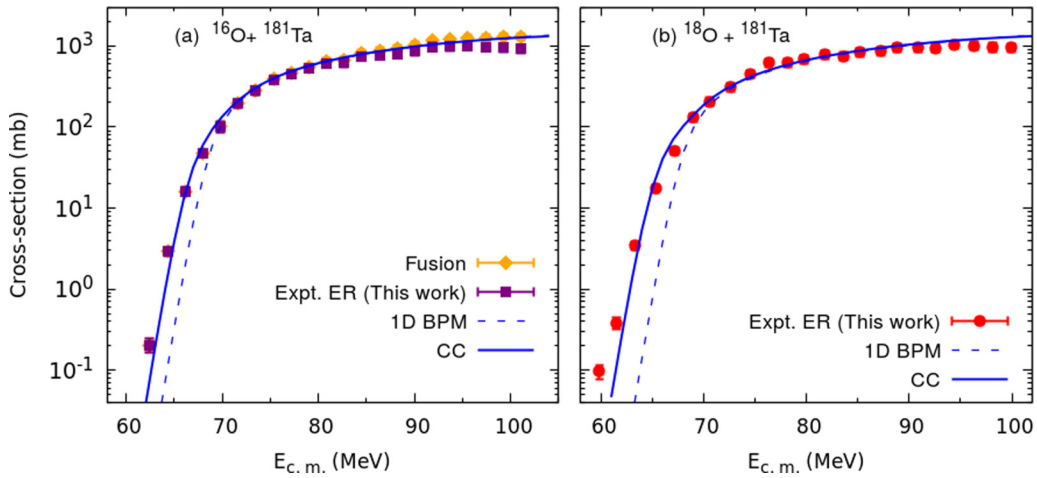

FIG. 2. Measured ER excitation function as a function of $E_{\mathrm{c.m.}}$ for $^{16,18}\mathrm{O} + {}^{181}\mathrm{Ta}$ reactions along with CC calculations. Solid line represents CC calculations with coupling and dashed line that without coupling (see text for coupling details).

the weighted average was estimated using statistical code PACE4 [39]. The average HIRA efficiency values generally have ≈10% uncertainty.

Another matter of considerable importance is the identification of ER at the focal plane detector. This was achieved by the simultaneous measurement of energy loss, ΔE (measured at the cathode of MWPC) and time of flight (TOF) of the ERs, which will provide a clear separation of ERs from projectilelike background events. This time-of-flight spectrum was generated by taking the start signal from the MWPC anode and the stop signal from the rf of the beam. The scatter plot of ΔE versus TOF at $E_{\mathrm{lab}} = 94.0$ MeV ($E_{\mathrm{c.m.}} = 86.15$ MeV) for the reaction $^{16}\mathrm{O} + {}^{181}\mathrm{Ta}$ is shown in Fig. 1. At lower beam energies, a "blank" target run was used to estimate background at the focal plane of HIRA. Such a background correction was introduced for the low energy measurements. The ER cross sections obtained for $^{16,18}\mathrm{O} + {}^{181}\mathrm{Ta}$ reactions after the data reduction are given in Table I and Fig. 2. Overall error was estimated to be $\leqslant 15\%$ and the major part is from ϵ_{HIRA}.

IV. RESULTS AND DISCUSSION

A nucleus is a many-body quantum-mechanical system with a large number of degrees of freedom. The challenge lies in whether to consider these degrees of freedom statistically or exactly. At lower excitation energies considering different degrees of freedoms such as collective surface vibration, deformation of colliding nuclei and neutron transfer, and coupled channels calculation [39] explains the fusion cross section quite well. Nuclear fission and particle evaporation are the dominant modes of decay at higher excitation energies for heavy-ion collisions. Their excitation functions at energies well above the Coulomb barrier are weakly sensitive to the form of nuclear potential and are mainly determined by the standard statistical model parameters. In the present study, coupled channel calculations have been carried out to explore the effect of different coupling states of target and projectile below the Coulomb barrier energy region and statistical model calculations to understand the decay mechanisms in the higher excitation energies.

A. Coupled channels calculation

Coupled channels (CCs) calculations of $^{16,18}\mathrm{O} + {}^{181}\mathrm{Ta}$ were performed to determine the effect of projectile structure on ER cross sections in the energy region below the Coulomb barrier. A modified version of CCFULL code by Hagino *et al.* [39,40] is used in the present analysis for CC calculations. Woods-Saxon parameters like depth of potential (V_0), radius (r_0), and diffuseness (a) for coupled channel calculations are selected from that of the nearest system $^{16}\mathrm{O} + {}^{186}\mathrm{W}$ [41]. The parameters V_0, r_0, and a are fixed as 92.25 MeV, 1.15 fm, and 0.73 fm, respectively to produce a fusion barrier which is equal to the experimental fusion barrier of $^{16}\mathrm{O} + {}^{181}\mathrm{Ta}$ reaction. The CCFULL calculations with these potential parameters without including any coupling is termed as a one-dimensional barrier penetration model (1D BPM) calculations. We have used the same potential parameters for both $^{16,18}\mathrm{O} + {}^{181}\mathrm{Ta}$ reactions. Further, coupling with quadrupole ($\beta_2 = 0.262$ [42]) and hexadecapole ($\beta_4 = -0.091$ [43]) deformations of ^{181}Ta target nuclei explained the subbarrier fusion enhancement of the $^{16}\mathrm{O} + {}^{181}\mathrm{Ta}$ reaction in the below-barrier energy region. Coupled channel calculations including the 3^- state of ^{16}O having 6.130 MeV and $\beta_3 = 0.729$ substantially overestimate the experimental excitation function. Such behavior was observed by Hagino *et al.* [44] in the analysis of $^{16}\mathrm{O} + {}^{144}\mathrm{Sm}$, while including the octupole vibration of ^{16}O in CC calculation. Furthermore, by treating ^{16}O as inert, they explained the experimental cross sections and barrier distributions satisfactorily. This was attributed to an adiabatic coupling which introduces a static point shift and mass renormalization [44]. On including the first 2^+ vibrational state of ^{18}O and the first rotational state of ^{181}Ta, CC calculations explained the excitation function of $^{18}\mathrm{O} + {}^{181}\mathrm{Ta}$ reaction in the below barrier region. The deformation parameters and excitation

TABLE II. Deformation parameters and first excitation energies of different nuclei used in the coupled channel calculation.

Nucleus	Energy of 1st ex. state (MeV)	β_2	β_4	Ref.
^{181}Ta	0.0967	0.262	−0.091	[42,43]
^{18}O	1.982	0.355		[45]

energies used in the coupled channel calculations are listed in Table II.

The experimental ER excitation functions and results of the CCFULL calculations of ^{16,18}O + ^{181}Ta reactions respectively are shown in Figs. 2(a) and 2(b). In Fig. 2(a) the 1D BPM calculations explain the fusion cross section well in the above-barrier region. The couplings of the relative motion of the colliding nuclei with the vibration of projectile and the rotation of target nuclei explains the cross sections in the below-barrier energy region for both the reactions. However, at $E_{\rm c.m.} = 59.85$ MeV of the ^{18}O + ^{181}Ta reaction, experimental cross sections show a deviation from coupled channel calculations. Inclusion of the rotational and vibrational degree of freedom is found to be not sufficient to explain the enhancement in subbarrier fusion cross sections of ^{16}O + ^{181}Ta. This indicates the need for including additional transfer channel in the CC calculations. When systems of two colliding nuclei have positive Q values for any transfer channel, they are found to exhibit enhancement in subbarrier fusion due to neutron rearrangement [46,47]. A $2n$ transfer channel of ^{18}O + ^{181}Ta reaction has a transfer Q value of +0.809 MeV and in the case of ^{16}O + ^{181}Ta, it is −15.89 MeV. Accordingly, we may attribute the observed enhancement in subbarrier cross sections for ^{18}O + ^{181}Ta to a positive $2n$ transfer channel.

B. Statistical model calculations

In the present work, we have used the HIVAP [10,15] code to describe experimental cross sections above the Coulomb barrier energy region. In HIVAP, a potential barrier passing model incorporated with a standard statistical model is used to investigate the nuclear reactions. The HIVAP code with a standard set of parameters, which is referred to as the Reisdorf and Schadel parameters [10], is used for calculations. In the statistical model analysis, ER excitation functions well above the fusion barrier energies are insensitive to the choice of nuclear potential [16]. Among the various input parameters of the HIVAP code, the cross-section calculations are most sensitive to the choice of SSM parameters such as the depth of the fission barrier (B_f) and the ratio of the level densities at the saddle point to that of equilibrium deformation (a_f/a_n). According to Reisdorf formula, the nuclear level density leads to a ratio $a_f/a_n \gtrsim 1$, due to the different nuclear shapes at fission and particle emission states [15]. Shell correction energy which is associated with exponentially varying excitation energy, with damping constant 18.5 [16], is taken into account while calculating level densities. At energies well above the fusion barrier, statistical model calculation results depend mainly on k_f, which relates to the fission barrier [$B_f(\ell)$] by the expression

$$B_f(\ell) = k_f\, B_f^{\rm LD}(\ell) + \delta W_{\rm gs}. \tag{2}$$

Here $B_f^{\rm LD}(\ell)$ is the rotating liquid drop model fission barrier [48] and $\delta W_{\rm gs}$ is the ground state shell correction, which is calculated as the difference between empirical [49] and liquid drop masses [14].

For heavy systems, NCNF processes like fast fission and quasifission are possible. Among these, quasifission was reported for many heavy-ion induced reactions, especially in the actinide region [50]. Despite extensive works on NCNF processes [51] in preactinide as well as actinide regions, it is not clearly understood whether NCNF is always associated with suppression of the formation of ER.

Based on the $\alpha/\alpha_{\rm BG}$ criterion, the present reactions can be classified as ^{16}O + ^{181}Ta with $\alpha/\alpha_{\rm BG} > 1$ (absence of NCNF) and ^{18}O + ^{181}Ta with $\alpha/\alpha_{\rm BG} < 1$ (presence of NCNF). Therefore, contributions to ER cross-section values from both reactions are expected to be different. However, experimentally both reactions show almost the same $\sigma_{\rm ER}$ values in the above-barrier region. This indicates the absence of the direct signature of QF (that is the reduction in ER excitation function) in ^{18}O + ^{181}Ta with respect to a more asymmetric ^{16}O + ^{181}Ta reaction.

Statistical model calculations using HIVAP are carried out to search for the presence of noncompound nuclear fission processes. In HIVAP calculations, at higher energies, default values of parameters are kept as suggested by Reisdorf and Schädel [10]. HIVAP calculations with $P_{\rm CN} = 1$ and $k_f = 1$ reproduce fission cross sections of ^{16}O + ^{181}Ta reaction [52,53] at $E_{\rm lab} = 115$, 120 MeV ($E_{\rm c.m.} = 105.65$, 110.25 MeV) energies only. Further, reduction of k_f up to 0.9 with $P_{\rm CN} = 1$ was needed to explain all the fission cross sections of the ^{16}O + ^{181}Ta reaction. Thus, the experimental fission cross sections of the ^{16}O + ^{181}Ta reaction, reported by Videbæk *et al.* [52] and Behera *et al.* [53], were reproduced by the HIVAP calculations with $k_f = 0.9$–1.0. Also, corresponding ER cross sections from HIVAP calculations reproduced the experimental ER excitation function of ^{16}O + ^{181}Ta. The value of k_f in this range (0.9–1.0), which reproduces all the experimental fission cross-sections, is taken as the fission barrier scaling factor for the ^{16}O + ^{181}Ta reaction. Accordingly, we select $k_f = 0.95 \pm 0.05$ for the ^{16}O + ^{181}Ta reaction. ER and fission excitation functions with $k_f = 0.95$ are represented by blue solid and dashed lines, respectively, in Fig. 3(a). Also, ER and fission excitation functions in the said range of k_f (0.9–1.0) are shown as colored bands. Behera *et al.* [53] performed statistical model calculations with $k_f = 0.99$ and $a_f/a_n = 1.012$ for the ^{16}O + ^{181}Ta reaction and reported the absence of quasifission below and above barrier energy points. They could reproduce the fission excitation function and prescission neutron multiplicity data with $k_f = 0.99$ [53], which is within the range we observed.

ER excitation function of ^{16}O + ^{181}Ta measured by Singh *et al.* [54] is also shown (brown open squares) in Fig. 3(a) along with the present data. It is evident that measurements made by Singh *et al.* [54] show lower values for cross sections compared to that of our ^{16}O + ^{181}Ta. They have used

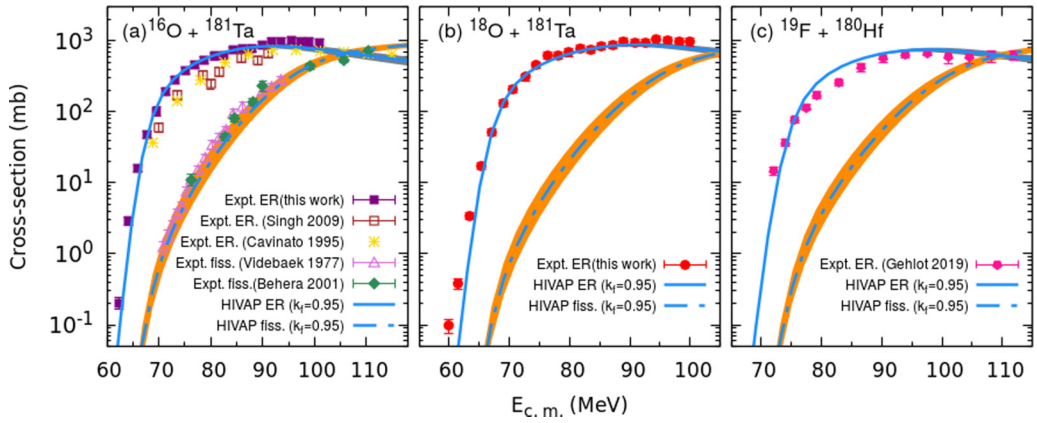

FIG. 3. Experimental ER and fission excitation functions for (a) ^{16}O + ^{181}Ta, (b) ^{18}O + ^{181}Ta, and (c) ^{19}F + ^{180}Hf [35] reactions along with HIVAP calculations. Excitation functions for a range of k_f (0.9–1) are represented by bands. In (a), the green diamond and violet open triangles represent fission cross sections, taken from [53] and [52] respectively. Also, ER cross sections measured by [54] and [55] are shown as brown open squares and yellow asterisk symbols respectively.

gamma-ray activation technique for measurements of ER excitation functions and included only activities corresponding to $3n$, $4n$, and $5n$ channels [54]. Cavinato *et al.* [55] also measured cross sections of fusion without fission for the same projectile-target combinations [as represented by yellow asterisk symbol in Fig. 3(a)]. They limited their measurements to $^{189-193}$Tl, $^{189-193}$Hg, ^{189,191}Pt nuclei as ERs and excluded ^{194}Tl. ^{194}Tl, the $3n$ exit channel, as per statistical model calculation contributes a major part for the below barrier cross section. The absence of ^{194}Tl channel in Cavinato's data [55] could be the reason for the observed deviation between their data and the present measurements.

In order to find the threshold value of mass asymmetry in the $A \approx 200$ region, two reactions induced by ^{18}O and ^{19}F which form the same CN ^{199}Tl are considered. To bring about the starting point of the NCNF reaction in less fissile Tl, k_f is fixed by the most asymmetric reaction ^{18}O + ^{181}Ta. The ^{16}O + ^{181}Ta reaction is considered as a compound nucleus fission (CNF) type reaction based on the systematics of Banerjee *et al.* [29] and it has an $\alpha > \alpha_{BG}$. As the two reactions (^{16}O + ^{181}Ta, ^{18}O + ^{181}Ta) differ only by two neutrons in the projectile, we have used the same $k_f = 0.95$ for ^{18}O + ^{181}Ta with the same set of HIVAP parameters. Experimental cross sections of both ^{16,18}O + ^{181}Ta reactions are in agreement with HIVAP calculations with $k_f = 0.95 \pm 0.05$ and $P_{CN} = 1$, which indicates the absence of quasifission in both reactions. Colored bands in Fig. 3(b) show the excitation functions of ^{18}O + ^{181}Ta in the entire range of k_f (0.9–1.0).

To search for the presence of NCNF reactions in ^{19}F + ^{180}Hf [35], first we tried to reproduce ER excitation function of the same, with the parameter set used to calculate the ^{18}O + ^{181}Ta reaction. ER excitation functions of ^{19}F + ^{180}Hf, from the HIVAP calculation with k_f 0.9–1.0 ($P_{CN} = 1$) were found to be within the errors of experimental ER excitation function as shown in Fig. 3(c). Scaling in P_{CN} is not required to have a better agreement with the experimental cross sections. Some experimental points at around the barrier show small but a notable deviation from statistical model calculations, which needs further study. $P_{CN} = 1$ in all the three reactions mentioned in this discussion explains the ER excitation function well, irrespective of their entrance channel mass asymmetry. This $P_{CN} = 1$ does not allow us to predict quasifission like NCNF reactions in these systems. Any further predictions with smaller k_f value for ^{19}F + ^{180}Hf require fission data which are currently not available. No fusion suppression effects are found for both reactions as far as P_{CN} values are concerned. Surely, it should be confirmed through fission experiments of ^{19}F + ^{180}Hf that the fusion suppression really exists for less fissile systems induced by ^{19}F.

Banerjee *et al.* [29] have shown the variation of P_{CN} with entrance channel mass asymmetry α, charge product $Z_P Z_T$, and compound nucleus fissility χ_{CN}. They found a boundary for χ_{CN} (which is related with $Z_P Z_T$ and α) where P_{CN} starts to deviate from unity in the $A \approx 200$ region. The systems ^{16,18}O + ^{181}Ta ($Z_P Z_T = 584$), ^{19}F + ^{180}Hf ($Z_P Z_T = 648$) with $\alpha = 0.8376, 0.8314, 0.8090$ ($\alpha = \frac{A_t - A_p}{A_t + A_p}$) and $\chi_{CN} = 0.6936, 0.6905$, respectively, lie below this limit of χ_{CN}, indicating the absence of NCNF in these reactions. In other words, the calculations using HIVAP and the systematics reported by Banerjee *et al.* [29] come to the same conclusion regarding the presence of quasifission in the measured reactions.

Also, Singh *et al.* [56] compared the neutron multiplicity data of ^{16}O + ^{181}Ta and ^{19}F + ^{178}Hf reactions which form the same CN ^{197}Tl. Since the time scale for QF is small compared to fusion fission, it is expected that average prescission neutron multiplicity will be higher for reactions with QF. Prescission neutron multiplicity of ^{19}F + ^{178}Hf shows an increase with excitation energy with a larger rate as compared to ^{16}O + ^{181}Ta. However, an increasing rate of dissipation strength of ^{19}F + ^{178}Hf does not allow enhancement of neutron multiplicity to assimilate solely with QF. This also validates our observation; the absence of any signature of QF in ^{19}F induced less fissile reactions.

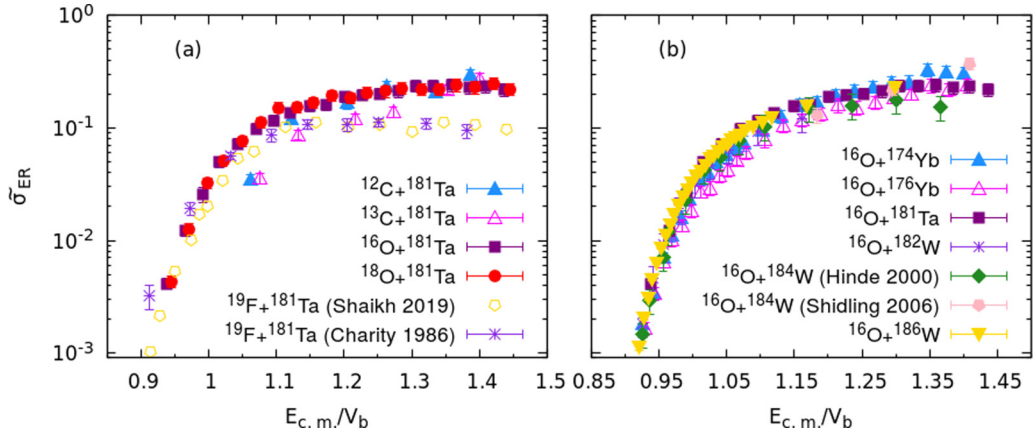

FIG. 4. Reduced cross sections as a function of $E_{c.m.}/V_b$ for reactions forming CN in $A \approx 200$ region. Here reduced cross section is obtained by dividing absolute cross section with πR_b^2, where R_b is the barrier radius and V_b is the Bass barrier. The ER cross sections of $^{12,13}C + ^{181}Ta$ [60], $^{19}F + ^{181}Ta$ (Refs. [42] and [61]), $^{16}O + ^{174,176}Yb$ [57], $^{16}O + ^{182}W$ [58], $^{16}O + ^{184}W$ (Refs. [59] and [58]), and $^{16}O + ^{186}W$ [62] are obtained from the literature.

C. General remarks

ER measurements of additional systems which form CN near Tl nuclei are considered for comparison with the present data, and are shown in Figs. 4(a) and 4(b). Most of these systems form CN in the preactinide ($A \approx 200$) region. In order to verify the effects of different projectiles on the ^{181}Ta target, we compared the reduced cross sections ($\tilde{\sigma}_{ER} = \pi R_b^2$, where R_b is the barrier radius) of $^{16,18}O + ^{181}Ta$ reactions with that of different projectiles as shown in Fig. 4(a). Cross sections of all selected reactions fall almost in the same cross-section region. A minor increase is observed in ^{12}C reactions, which may be due to the cluster structure properties of ^{12}C [60]. Among these reactions, $^{19}F + ^{181}Ta$ shows a significant reduction in cross section, which might be attributed to the presence of noncompound nuclear fission reactions [33]. Further comparison of reduced cross sections of ^{16}O on various targets is shown in Fig. 4(b). In the observed energy range, all reactions fall in the same cross-section region. From these comparisons of reduced cross sections, it is evident that the reactions involving less fissile CN do not show any direct entrance channel effect except for certain projectiles such as ^{19}F.

In Table III, we list the systems near the Tl compound nucleus [13,16,23,34] along with present reactions. $\frac{\alpha}{\alpha_{BG}} < 1$ predicts the presence of quasifission in some reactions listed in the Table III. However, their $P_{CN} = 1$ show the absence of NCNF. Thus α and α_{BG} values cannot be used to accurately

TABLE III. The table lists reactions considered in $A \approx 200$ region and their charge product $Z_P Z_T$, neutron number of compound nuclei N_{CN}, fission barrier scaling factor k_f, the ratio of mass asymmetry values and its critical value at BG point $\frac{\alpha}{\alpha_{BG}}$ [30], and fusion probability P_{CN}. Two values of k_f and P_{CN} correspond to variations in those numbers with different fits.

Reaction	N_{CN}	$Z_P Z_T$	$\frac{\alpha}{\alpha_{BG}}$	k_f	P_{CN}	Ref.
$^{12}C + ^{208}Pb \rightarrow ^{220}Ra$	132	492	1.0334	0.85 [23]	1	[23]
$^{12}C + ^{206}Pb \rightarrow ^{218}Ra$	130	492	1.0307	0.82 [23]	1	[23]
$^{19}F + ^{197}Au \rightarrow ^{216}Ra$	128	711	0.9528	[0.78,0.82] [23]	[1,0.65]	[63]
$^{12}C + ^{204}Pb \rightarrow ^{216}Ra$	128	492	1.0277	0.82 [23]	1	[23]
$^{19}F + ^{198}Pt \rightarrow ^{217}Fr$	130	702	0.9613	[0.78,0.85] [25]	[1,0.73]	[64]
$^{18}O + ^{197}Au \rightarrow ^{215}Fr$	128	632	0.9687	0.85 [13]	1	[13]
$^{19}F + ^{194}Pt \rightarrow ^{213}Fr$	126	702	0.9542	[0.78,0.82] [25]	[1,0.75]	[64]
$^{16}O + ^{197}Au \rightarrow ^{213}Fr$	126	632	0.9870	0.82 [13]	1	[65]
$^{18}O + ^{192}Os \rightarrow ^{210}Po$	126	608	0.9820	0.92 [16]	1	[65]
$^{16}O + ^{192}Os \rightarrow ^{208}Po$	124	608	1.0009	0.88 [16]	1	[66]
$^{18}O + ^{188}Os \rightarrow ^{206}Po$	122	608	0.9742	0.82 [16]	1	[66]
$^{16}O + ^{188}Os \rightarrow ^{204}Po$	120	608	0.9934	0.77 [16]	1	[66]
$^{16}O + ^{186}W \rightarrow ^{202}Pb$	120	592	1.0065	0.85 [34]	1	[67]
$^{19}F + ^{181}Ta \rightarrow ^{200}Pb$	118	657	0.9666	0.85 [34]	1	[61]
$^{16}O + ^{184}W \rightarrow ^{200}Pb$	118	592	1.0024	0.85 [34]	1	[68]
$^{19}F + ^{180}Hf \rightarrow ^{199}Tl$	118	648	0.9731	0.95[This work]	1	[35]
$^{18}O + ^{181}Ta \rightarrow ^{199}Tl$	118	584	0.9852	0.95	1	this work
$^{16}O + ^{181}Ta \rightarrow ^{197}Tl$	116	584	1.0051	0.95	1	this work

predict the presence of NCNF in experimental cases involving less fissile systems. For systems forming Fr, Ra compound nuclei, k_f shows an increase with the increase in N_{CN} (beyond $N = 126$ shell closure), as can be seen in Table III. In systems forming Po nuclei, which are listed in Table III, such proportionate increase in k_f with N_{CN} is observed before $N = 126$ [16]. Further, it may be concluded from Table III that at the nearby region of the BG point, k_f shows an increase with neutron number irrespective of $N = 126$ shell closures. Also, mass asymmetry values do not play much of a role in fusion suppression in this region. A more thorough analysis is needed in this region to have a better insight into the interplaying effects.

V. SUMMARY AND CONCLUSION

We have measured the ER excitation function for ^{16,18}O + ^{181}Ta leading to the compound nuclei ^{197}Tl and ^{199}Tl respectively, using a recoil mass spectrometer. Comparisons of α and α_{BG} values predicted quasifission in the ^{18}O + ^{181}Ta reaction and no such process in ^{16}O + ^{181}Ta. However, no specific signatures of fusion suppression due to QF were found in the ER excitation function of the less asymmetric ^{18}O + ^{181}Ta ($\alpha < \alpha_{BG}$) reaction in comparison with the more asymmetric ^{16}O + ^{181}Ta ($\alpha > \alpha_{BG}$). Also, we have analyzed the measured evaporation residue cross sections using the statistical model code HIVAP. For both reactions, the ER excitation functions are well reproduced by HIVAP calculation with the same fission barrier scaling factor k_f and P_{CN}, which indicates the absence of NCNF. For ^{220}Th CN forming reactions Mandaglio *et al*. [69] reported a strong sensitivity for entrance channel asymmetry with the exit channel. However, a comparison between ^{18}O + ^{181}Ta and ^{19}F + ^{180}Hf [35] forming ^{199}Tl reactions shows no such strong sensitivity. This may be due to the lower value of fissility of the systems or due to high resemblance in mass asymmetry. Attempts to search for a starting point of the fusion suppression in the $A \approx 200$ region in highly fissile CN give us some indirect evidence of the effects such as the lowering of P_{CN} from 1. More precise experiments that explore combinations leading to the same CN are required for better insight.

ACKNOWLEDGMENTS

We are grateful to the Pelletron group of IUAC for providing an excellent beam of required pulse width throughout the experiment. We are indebted for the support received from the target and data support laboratories of IUAC. One of the authors (P.J.) acknowledges the financial support from the University Grants Commission (UGC), India, in the form of a BSR fellowship.

[1] J. H. Hamilton, S. Hofmann, and Y. T. Oganessian, Annu. Rev. Nucl. Part. Sci. **63**, 383 (2013).
[2] Y. T. Oganessian and V. K. Utyonkov, Rep. Prog. Phys. **78**, 036301 (2015).
[3] A. Shamlath, E. Prasad, N. Madhavan, P. V. Laveen, J. Gehlot, A. K. Nasirov, G. Giardina, G. Mandaglio, S. Nath, T. Banerjee, A. M. Vinodkumar, M. Shareef, A. Jhingan, T. Varughese, DVGRKS Kumar, P. S. Devi, Khushboo, P. Jisha, N. Kumar, M. M. Hosamani, and S. Kailas, Phys. Rev. C **95**, 034610 (2017).
[4] A. Shamlath, M. Shareef, E. Prasad, P. Sugathan, R. G. Thomas, A. Jhingan, S. Appannababu, A. K. Nasirov, A. M. Vinodkumar, K. M. Varier, C. Yadav, B. R. S. Babu, S. Nath, G. Mohanto, I. Mukul, D. Singh, and S. Kailas, Nucl. Phys. A **945**, 67 (2016).
[5] A. C. Berriman, D. J. Hinde, M. Dasgupta, C. R. Morton, R. D. Butt, and J. O. Newton, Nature (London) **413**, 144 (2001).
[6] J. Gehlot, A. M. Vinodkumar, N. Madhavan, S. Nath, A. Jhingan, T. Varughese, T. Banerjee, A. Shamlath, P. V. Laveen, M. Shareef, P. Jisha, P. S. Devi, G. N. Jyothi, M. M. Hosamani, I. Mazumdar, V. I. Chepigin, M. L. Chelnokov, A. V. Yeremin, A. K. Sinha, and B. R. S. Babu, Phys. Rev. C **99**, 034615 (2019).
[7] B. B. Back, H. Esbensen, C. L. Jiang, and K. E. Rehm, Rev. Mod. Phys. **86**, 317 (2014).
[8] M. Dasgupta, D. J. Hinde, N. Rowley, and A. M. Stefanini, Annu. Rev. Nucl. Part. Sci. **48**, 401 (1998).
[9] M. Dasgupta, D. J. Hinde, A. Diaz-Torres, B. Bouriquet, C. I. Low, G. J. Milburn, and J. O. Newton, Phys. Rev. Lett. **99**, 192701 (2007).
[10] W. Reisdorf and M. Schädel, Z. Phys. A **343**, 47 (1992).
[11] R. du Rietz, D. J. Hinde, M. Dasgupta, R. G. Thomas, L. R. Gasques, M. Evers, N. Lobanov, and A. Wakhle, Phys. Rev. Lett. **106**, 052701 (2011).
[12] D. J. Hinde, R. du Rietz, and M. Dasgupta, EPJ Web Conf. **17**, 04001 (2011).
[13] L. Corradi, B. R. Behera, E. Fioretto, A. Gadea, A. Latina, A. M. Stefanini, S. Szilner, M. Trotta, Y. Wu, S. Beghini, G. Montagnoli, F. Scarlassara, R. N. Sagaidak, S. N. Atutov, B. Mai, G. Stancari, L. Tomassetti, E. Mariotti, A. Khanbekyan, and S. Veronesi, Phys. Rev. C **71**, 014609 (2005).
[14] W. D. Myers and W. J. Swiatecki, Ark. Fys. **36**, 343 (1967).
[15] W. Reisdorf, Z. Phys. A **300**, 227 (1981).
[16] R. N. Sagaidak and A. N. Andreyev, Phys. Rev. C **79**, 054613 (2009).
[17] K. Banerjee, D. J. Hinde, M. Dasgupta, E. C. Simpson, D. Y. Jeung, C. Simenel, B. M. A. Swinton-Bland, E. Williams, I. P. Carter, K. J. Cook, H. M. David, C. E. Düllmann, J. Khuyagbaatar, B. Kindler, B. Lommel, E. Prasad, C. Sengupta, J. F. Smith, K. Vo-Phuoc, J. Walshe, and A. Yakushev, Phys. Rev. Lett. **122**, 232503 (2019).
[18] R. S. Naik, W. Loveland, P. H. Sprunger, A. M. Vinodkumar, D. Peterson, C. L. Jiang, S. Zhu, X. Tang, E. F. Moore, and P. Chowdhury, Phys. Rev. C **76**, 054604 (2007).
[19] V. Zagrebaev and W. Greiner, Phys. Rev. C **78**, 034610 (2008).
[20] W. Loveland, J. Phys.: Conf. Ser. **420**, 012004 (2013).
[21] K. Hagino, Phys. Rev. C **98**, 014607 (2018).
[22] D. J. Hinde, A. C. Berriman, R. D. Butt, M. Dasgupta, I. I. Gontchar, C. R. Morton, A. Mukherjee, and J. O. Newton, J. Nucl. Radiochem. Sci. **3**, 31 (2002).

[23] R. N. Sagaidak, G. N. Kniajeva, I. M. Itkis, M. G. Itkis, N. A. Kondratiev, E. M. Kozulin, I. V. Pokrovsky, A. I. Svirikhin, V. M. Voskressensky, A. V. Yeremin, L. Corradi, A. Gadea, A. Latina, A. M. Stefanini, S. Szilner, M. Trotta, A. M. Vinodkumar, S. Beghini, G. Montagnoli, F. Scarlassara *et al.*, Phys. Rev. C **68**, 014603 (2003).

[24] D. J. Hinde, M. Dasgupta, and A. Mukherjee, Phys. Rev. Lett. **89**, 282701 (2002).

[25] R. N. Sagaidak, A. Y. Chizhov, I. M. Itkis, M. G. Itkis, G. N. Kniajeva, N. A. Kondratiev, E. M. Kozulin, I. V. Pokrovsky, L. Corradi, E. Fioretto, A. Gadea, A. Latina, A. M. Stefanini, S. Beghini, G. Montagnoli, F. Scarlassara, M. Trotta, and S. Szilner, in *FUSION06: Reaction Mechanisms and Nuclear Structure at the Coulomb Barrier*, edited by L. Corradi, D. Ackermann, E. Fioretto, A. Gadea, F. Haas, G. Pollarolo, F. Scarlassara, S. Szilner, and M. Trotta , AIP Conf. Proc. No. 853 (AIP, Melville, NY, 2006), p. 114.

[26] R. Rafiei, R. G. Thomas, D. J. Hinde, M. Dasgupta, C. R. Morton, L. R. Gasques, M. L. Brown, and M. D. Rodriguez, Phys. Rev. C **77**, 024606 (2008).

[27] G. N. Knyazheva, E. M. Kozulin, R. N. Sagaidak, A. Y. Chizhov, M. G. Itkis, N. A. Kondratiev, V. M. Voskressensky, A. M. Stefanini, B. R. Behera, L. Corradi, E. Fioretto, A. Gadea, A. Latina, S. Szilner, M. Trotta, S. Beghini, G. Montagnoli, F. Scarlassara, F. Haas, N. Rowley *et al.*, Phys. Rev. C **75**, 064602 (2007).

[28] C. Schmitt, K. Mazurek, and P. N. Nadtochy, Phys. Rev. C **100**, 064606 (2019).

[29] T. Banerjee, S. Nath, and S. Pal, Phys. Rev. C **91**, 034619 (2015).

[30] U. L. Businaro and S. Gallone, Nuovo Cimento **5**, 315 (1957).

[31] P. Sharma, B. R. Behera, R. Mahajan, M. Thakur, G. Kaur, K. Kapoor, K. Rani, N. Madhavan, S. Nath, J. Gehlot, R. Dubey, I. Mazumdar, S. M. Patel, M. Dhibar, M. M. Hosamani, Khushboo, N. Kumar, A. Shamlath, G. Mohanto, and S. Pal, Phys. Rev. C **96**, 034613 (2017).

[32] V. Singh, B. R. Behera, M. Kaur, A. Kumar, K. P. Singh, N. Madhavan, S. Nath, J. Gehlot, G. Mohanto, A. Jhingan, I. Mukul, T. Varughese, J. Sadhukhan, S. Pal, S. Goyal, A. Saxena, S. Santra, and S. Kailas, Phys. Rev. C **89**, 024609 (2014).

[33] A. Nasirov, G. Mandaglio, M. Manganaro, A. Muminov, G. Fazio, and G. Giardina, Phys. Lett. B **686**, 72 (2010).

[34] R. Sagaidak, G. Kniajeva, I. Itkis, M. G. Itkis, N. A. Kondratiev, E. M. Kozulin, I. V. Pokrovsky, V. M. Voskressensky, A. Yeremin, L. Corradi, A. Gadea, A. Latina, A. Stefanini, S. Szilner, M. Trotta, A. M. Vinodkumar, S. Beghini, G. Montagnoli, F. Scarlassara, and N. Rowley, in *10th International Conference on Nuclear Reaction Mechanism, June 9–13, 2003, Varenna, Italy* (JINR, 2003).

[35] J. Gehlot, S. Nath, T. Banerjee, I. Mukul, R. Dubey, A. Shamlath, P. V. Laveen, M. Shareef, Md. Moin Shaikh, A. Jhingan, N. Madhavan, T. Rajbongshi, P. Jisha, and S. Pal, Phys. Rev. C **99**, 061601(R) (2019).

[36] A. Sinha, N. Madhavan, J. Das, P. Sugathan, D. Kataria, A. Patro, and G. Mehta, Nucl. Instrum. Methods Phys. Res. A **339**, 543 (1994).

[37] A. Jhingan and P. Sugathan, in *Proceedings of the DAE-BNRS Symposium on Nuclear Physics*, edited by S. R. Jain, P. Shukla, A. Chatterjee, and V. M. Datar (DAE-BRNS SNP, 2012), Vol. 57, pp. 138–145.

[38] S. Nath, Comput. Phys. Commun. **180**, 2392 (2009); **181**, 1659 (2010).

[39] A. Gavron, Phys. Rev. C **21**, 230 (1980); K. Hagino and N. Takigawa, Prog. Theor. Phys. **128**, 1061 (2012).

[40] K. Hagino, N. Rowley, and A. Kruppa, Comput. Phys. Commun. **123**, 143 (1999).

[41] M. Firihu, K. Hagino, and N. Takigawa, in *FUSION06: Reaction Mechanisms and Nuclear Structure at the Coulomb Barrier*, AIP Conf. Proc. No. 853, p. 309 (Ref. [25]).

[42] M. M. Shaikh, S. Nath, J. Gehlot, T. Banerjee, I. Mukul, R. Dubey, A. Shamlath, P. V. Laveen, M. Shareef, A. Jhingan, N. Madhavan, T. Rajbongshi, P. Jisha, G. N. Jyothi, A. Tejaswi, R. N. Sahoo, and A. Rani, J. Phys. G: Nucl. Part. Phys. **45**, 095103 (2018).

[43] P. Möller, A. J. Sierk, T. Ichikawa, and H. Sagawa, At. Data Nucl. Data Tables **109-110**, 1 (2016).

[44] K. Hagino, N. Takigawa, M. Dasgupta, D. J. Hinde, and J. R. Leigh, Phys. Rev. Lett. **79**, 2014 (1997).

[45] S. Ramen, C. W. Nestor, and P. Tikkanen, At. Data Nucl. Data Tables **78**, 1 (2001).

[46] G. L. Zhang, X. X. Liu, and C. J. Lin, Phys. Rev. C **89**, 054602 (2014).

[47] V. I. Zagrebaev, Phys. Rev. C **67**, 061601(R) (2003).

[48] A. J. Sierk, Phys. Rev. Lett. **55**, 582 (1985).

[49] G. Audi and A. H. Wapstra, Nucl. Phys. A **595**, 409 (1995).

[50] S. Kailas, J. Phys. G: Nucl. Part. Phys. **23**, 1227 (1997).

[51] R. Tripathi, S. Sodaye, and K. Sudarshan, Pramana **85**, 315 (2015).

[52] F. Videbæk, R. B. Goldstein, L. Grodzins, S. G. Steadman, T. A. Belote, and J. D. Garrett, Phys. Rev. C **15**, 954 (1977).

[53] B. R. Behera, S. Jena, M. Satpathy, S. Roy, P. Basu, M. K. Sharan, M. L. Chatterjee, S. Kailas, K. Mahata, and S. K. Datta, Phys. Rev. C **66**, 047602 (2002).

[54] D. P. Singh, Unnati, P. P. Singh, A. Yadav, M. K. Sharma, B. P. Singh, K. S. Golda, R. Kumar, A. K. Sinha, and R. Prasad, Phys. Rev. C **80**, 014601 (2009).

[55] M. Cavinato, E. Fabrici, E. Gadioli, E. Gadioli Erba, P. Vergani, M. Crippa, G. Colombo, I. Redaelli, and M. Ripamonti, Phys. Rev. C **52**, 2577 (1995).

[56] H. Singh, A. Kumar, B. R. Behera, I. M. Govil, K. S. Golda, P. Kumar, A. Jhingan, R. P. Singh, P. Sugathan, M. B. Chatterjee, S. K. Datta, Ranjeet, S. Pal, and G. Viesti, Phys. Rev. C **76**, 044610 (2007); H. Singh, A. Kumar, B. R. Behera, G. Singh, I. M. Govil, K. S. Golda, P. Kumar, A. Jhingan, R. P. Singh, P. Sugathan, M. B. Chatterjee, S. K. Datta, Ranjeet, S. Pal, and G. Viesti, *ibid.* **80**, 019909(E) (2009).

[57] T. Rajbongshi, K. Kalita, S. Nath, J. Gehlot, T. Banerjee, I. Mukul, R. Dubey, N. Madhavan, C. J. Lin, A. Shamlath, P. V. Laveen, M. Shareef, N. Kumar, P. Jisha, and P. Sharma, Phys. Rev. C **93**, 054622 (2016).

[58] D. J. Hinde, W. Pan, A. C. Berriman, R. D. Butt, M. Dasgupta, C. R. Morton, and J. O. Newton, Phys. Rev. C **62**, 024615 (2000).

[59] P. D. Shidling, N. M. Badiger, S. Nath, R. Kumar, A. Jhingan, R. P. Singh, P. Sugathan, S. Muralithar, N. Madhavan, A. K. Sinha, S. Pal, S. Kailas, S. Verma, K. Kalita, S. Mandal, R. Singh, B. R. Behera, K. M. Varier, and M. C. Radhakrishna, Phys. Rev. C **74**, 064603 (2006).

[60] K. S. Babu, R. Tripathi, K. Sudarshan, B. D. Shrivastava, A. Goswami, and B. S. Tomar, J. Phys. G: Nucl. Part. Phys. **29**, 1011 (2003).

[61] R. J. Charity, J. R. Leigh, J. J. M. Bokhorst, A. Chatterjee, G. S. Foote, D. J. Hinde, J. O. Newton, S. Ogaza, and D. Ward, Nucl. Phys. A **457**, 441 (1986).

[62] M. Trotta, A. M. Stefanini, S. Beghini, B. R. Behera, A. Yu. Chizhov, L. Corradi, S. Courtin, E. Fioretto, A. Gadea, P. R. S. Gomes *et al.*, Eur. J. Phys. A **25**, 615 (2005).

[63] R. Tripathi, K. Sudarshan, S. Sodaye, A. V. R. Reddy, K. Mahata, and A. Goswami, Phys. Rev. C **71**, 044616 (2005).

[64] K. Mahata, S. Kailas, A. Shrivastava, A. Chatterjee, P. Singh, S. Santra, and B. S. Tomar, Phys. Rev. C **65**, 034613 (2002).

[65] D. J. Hinde, R. J. Charity, G. S. Foote, J. R. Leigh, J. O. Newton, S. Ogaza, and A. Chattejee, Nucl. Phys. A **452**, 550 (1986).

[66] J. van der Plicht, H. C. Britt, M. M. Fowler, Z. Fraenkel, A. Gavron, J. B. Wilhelmy, F. Plasil, T. C. Awes, and G. R. Young, Phys. Rev. C **28**, 2022 (1983).

[67] R. C. Lemmon, J. R. Leigh, J. X. Wei, C. R. Morton, D. J. Hinde, J. O. Newton, J. C. Mein, M. Dasgupta, and N. Rowley, Phys. Lett. B **316**, 32 (1993).

[68] J. R. Leigh, J. J. M. Bokhorst, D. J. Hinde, and J. O. Newton, J. Phys. G: Nucl. Part. Phys. **14**, L55 (1988).

[69] G. Mandaglio, A. Anastasi, F. Curciarello, G. Fazio, G. Giardina, and A. K. Nasirov, Phys. Rev. C **98**, 044616 (2018).